

9 The Distance Scale of the Universe

Wendy L. Freedman · Barry F. Madore
Carnegie Observatories, Pasadena, CA, USA

1	<i>Introduction</i>	424
2	<i>Measurement of Distances</i>	425
3	<i>Parallaxes</i>	425
4	<i>Rotational Parallax Method</i>	426
5	<i>The Role of the Large and Small Magellanic Clouds</i>	426
6	<i>RR Lyrae Stars</i>	427
7	<i>Red Clump Stars</i>	430
7.1	The CMD Method, the Horizontal Branch, and Mira Variables	431
8	<i>Planetary Nebula Luminosity Function (PNLF)</i>	432
8.1	Globular Cluster Luminosity Functions (GCLF)	433
8.2	Novae	433
8.3	Type II Supernovae: EPM and SEAM	434
8.4	Cepheid Distance Scale	434
8.4.1	Galactic Cepheids with Trigonometric Parallaxes	435
9	<i>The Distance to the Large Magellanic Cloud Based on Cepheids</i>	436
9.1	Tip of the Red Giant Branch (TRGB) Method	437
9.2	Maser Galaxies	439
9.2.1	A Maser Distance to NGC 4258	439
9.2.2	Other Distance Determinations to NGC 4258	440
9.2.3	NGC 4258, UGC 3789, and Their Calibration of H_0	441
9.3	Surface Brightness Fluctuation (SBF) Method	441
9.4	Tully–Fisher Relation	442
9.5	Type Ia Supernovae	442
10	<i>The Extragalactic Distance Scale and the Hubble Constant</i>	445
	<i>Acknowledgments</i>	447
	<i>References</i>	447

Abstract: We critically review the methods currently being used to determine extragalactic distances. Within the Milky Way, direct parallaxes and traditional main-sequence fitting for both young open clusters and old globular clusters tie us directly to high-luminosity, variable stars used in extragalactic studies: Cepheids and RR Lyrae stars. These, in turn, inform a calibration of the tip of the red giant branch as well as red clump stars. Apart from the Milky Way, we focus on the Large Magellanic Cloud as an important stopping point at which a large variety of possible distance indicators have been evaluated and differentially tested against each other. Beyond the Local Group many stellar distance indicators fall below current detection and/or resolution limits, and they must be replaced with methods employing higher luminosity (and often much more rare) objects. These methods include the properties of nuclear masers, surface brightness fluctuations, the Tully–Fisher relation, and finally various types of supernovae. Ultimately a calibration of the expansion rate of the universe can provide distances using observed recessional velocities scaled by the Hubble constant.

1 Introduction

Modern extragalactic astronomy began with Edwin Hubble's discovery of Cepheid variables in NGC 6822 (Hubble 1925), M33 (Hubble 1926), and M31 (Hubble 1929). It has taken the better part of a century to develop the instrumentation and techniques to measure distances to accuracies of better than 10%, but this is now routine. Smith (1982) gives a history of the “Great Debate” that occupied the first three decades of the twentieth Century, while Webb (1999) gives a popular and very readable account of measuring the universe. Recent developments and a discussion of the convergence of the extragalactic distance to better than 10% accuracy are reviewed by Freedman and Madore (2010). The current article builds upon and augments this discussion. Previous accounts can be found in Hodge (1982), Rowan-Robinson (1985), Huchra (1992), Jacoby et al. (1992), van den Bergh (1992), Jackson (2007), and Tammann et al. (2008). There are also several conference proceedings dedicated to the extragalactic distance scale, including those edited by van den Bergh and Pritchet (1988) and by Livio et al. (1997); “Stellar Candles for the Extragalactic Distance Scale” edited by Alloin and Gieren (2003) is particularly comprehensive. Finally, a very up-to-date and authoritative account of distance measurements in astronomy has recently been published by de Grijs (2011).

Over the years, a great many extragalactic distance indicators have been tested, calibrated, and applied to nearby galaxies. Until recently these individual determinations have been scattered throughout the literature and were not being tracked or compiled in any systematic way. This has all changed with the introduction of NED-D, which is a feature of the NASA/IPAC Extragalactic Database (NED) that is dedicated to archiving published distances to galaxies, linking them back to the individual objects, and making them widely available in electronic form. These up-to-date compilations can be accessed on object-by-object basis through the main NED interface (<http://ned.ipac.caltech.edu/forms/d.html>), and the entire archive of distances can be downloaded as a single file from <http://ned.ipac.caltech.edu/Library/Distances/>. NED-D is updated several times a year.

2 Measurement of Distances

Measuring extragalactic distances generally involves use of one of two types of cosmological distances: the luminosity distance,

$$d_L = \sqrt{\frac{L}{4\pi F}} \quad (9.1)$$

which relates the observed flux (integrated over all frequencies), F , of an object to its intrinsic luminosity, L , emitted in its rest frame; and the angular diameter distance,

$$d_A = \frac{D}{\theta} \quad (9.2)$$

which relates the apparent angular size of an object in radians, θ , to its proper size, D . The luminosity and angular diameter distances are related by

$$d_L = (1 + z)^2 d_A. \quad (9.3)$$

The distance modulus, μ , is related to the luminosity distance as follows:

$$\mu \equiv m - M = 5 \log d_L - 5 \quad (9.4)$$

where m and M are the apparent and absolute magnitudes of the objects, respectively, and d_L is in units of parsecs.

Characterized as “standard candles” and “standard rulers,” or more generally known simply as “distance indicators,” methods that transcend geometry usually rely on identifying a quantity that is independent of distance (a color, a period, a morphological feature, etc.) that can be precisely measured and then shown to be a predictor of another property of the object in question (say a star or an entire galaxy) that is either dimmed in luminosity or reduced in size with distance.

3 Parallaxes

Measuring a parallax (i.e., using direct geometric triangulation with the annual displacement of the Earth around the Sun as a baseline) is the most straightforward way of determining interstellar distances. In principle, triangulation can be used over any distance; however, the level of precision required in its application is quickly outstripped by the increasing distances encountered across our Milky Way galaxy and beyond. Virtually all of the distances discussed from this point on build upon and use trigonometric parallaxes as foundational but generally rely on the inverse-square law fall-off of apparent luminosity with distance as the means of inferring distances across cosmic scales. A comprehensive review of trigonometric parallaxes and especially the impact of the Hipparcos astrometric satellite can be found in Heck and Caputo (1999), amplified and updated in Perryman (2009). We discuss the HST Cepheid parallax calibration in [Sect. 8.4.1](#).

4 Rotational Parallax Method

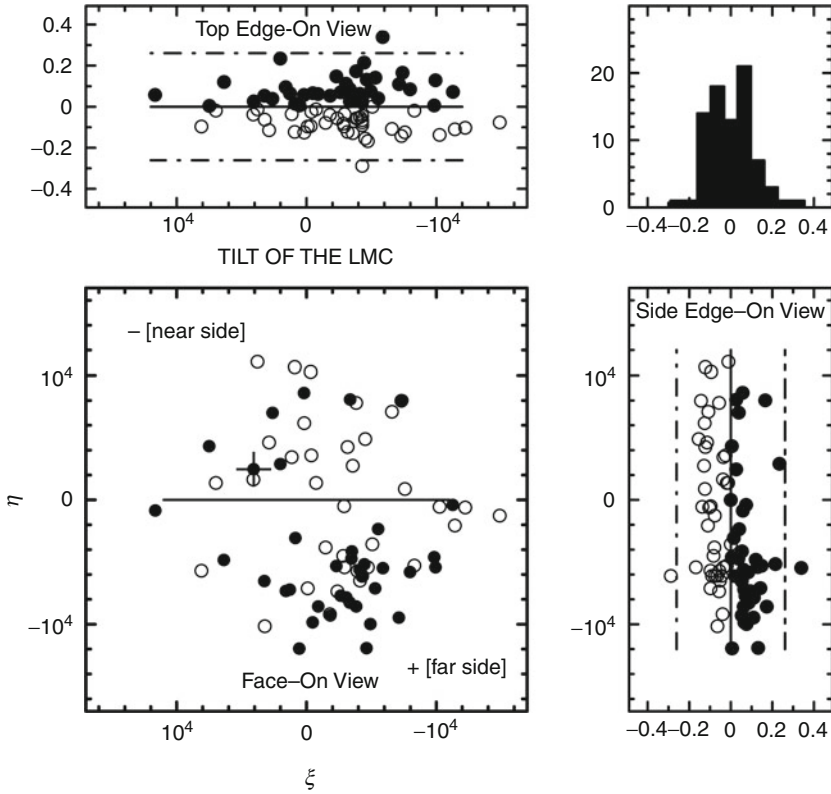
In a variety of contexts (optical and radio), the combination of proper motions and radial velocities has been implemented as a novel and promising means of determining a geometric distance to nearby galaxies (Loeb et al. 2005). For objects in the Local Group (at distances out to ~ 1 Mpc.), proper motions having a precision of 10–20 $\mu\text{arcsec}/\text{year}$ measured from the ground (in the radio) or from space (e.g., with the planned European Space Agency mission GAIA) are sufficient to provide “rotational parallaxes” within a 3–5-year time baseline. For a rotating disk galaxy (such as M31 or M33), the in-plane rotational velocity (km/s) can be equated to the transverse angular velocity (i.e., the proper motion) appropriately scaled by the distance. By measuring (tangential) proper motions and having knowledge of the radial-velocity field of the disk (corrected for inclination), one can derive the distance assuming reasonable symmetries in the structure of the disk and its velocity field.

Using 22 GHz H_2O (water) masers, a rotational parallax for M33 has already been measured (Brunthaler et al. 2005), and a complementary program is now underway using recently discovered water masers in M31 (Darling 2011). Water masers have also been observed in IC 10 (Henkel et al. 1986), but given their less than regular velocity field (Wilcots and Miller 1998), the inversion of proper motions and radial velocities to determine a distance to this galaxy will be more challenging. Perhaps the apparent angular divergence of sources (discussed by Darling 2011 for M31) as IC 10 approaches the Milky Way at -350 km/s, can be used in the future.

5 The Role of the Large and Small Magellanic Clouds

The Large Magellanic Cloud has played and probably will continue to play a central role in the refinement of the extragalactic distance scale. The primary reason is, of course, its proximity. Additionally, the LMC is a composite system, containing a mix of old, intermediate-age, and young stars in a system that is sufficiently massive that it has numerous examples of almost every type of distance indicator currently in use; one notable exception being a recent type Ia supernova. An extensive compilation of 275 distance estimates to the LMC is currently available from the NASA/IPAC Extragalactic Database (NED): <http://nedwww.ipac.caltech.edu/cgi-bin/nDistance?name=lmc>. The range in quoted distances is almost certainly dominated by systematic errors. The values for the LMC distance modulus fall generally in the range of 18.1–18.7 mag (i.e., 42–55 kpc), with more recent values tending to cluster around a distance modulus of 18.5 mag (see Alves 2004; Schaeffer 2008).

The LMC is sufficiently far away that its stellar components can all be considered to be at the same distance. Under this assumption, most of the observed dispersion in any luminosity-based distance indicator can be ascribed either to differential reddening or an intrinsic scatter in the distance determination method itself. Similarly, differences in relative zero points of various distance indicators when compared in a single system, like the LMC, can expose systematic errors in one or both of the methods. At a finer level of scrutiny, however, the back-to-front geometry of the LMC is in fact measurable by individual distance indicators of exceptionally high internal precision, such as the Classical Cepheids (Gascoigne and Shobbrook 1978), or by methods employing large statistical samples (e.g., Weinberg and Nikolaev 2001). Systematic shifts in the apparent distance modulus with position on the sky can then, with some certainty, be attributed to tilt of the disk of the galaxy with respect to the plane of the sky.



■ Fig. 9-1

The residuals in the Leavitt law at $3.6\ \mu\text{m}$ recently observed using Spitzer plotted as a function of position in the LMC (Scowcroft et al. 2012) from which the tilt of the LMC can be measured

◆ Figure 9-1 illustrates this for Cepheids in the LMC recently observed using mid-IR data Cepheid from Spitzer (Scowcroft et al. 2012).

The Small Magellanic Cloud is only slightly (0.4 mag or 10 kpc) further away than the LMC, and it is also somewhat less massive, but its three-dimensional geometry is so distorted that the system as a whole holds less promise than the LMC (or even some more distant galaxies like IC 1613, M31, and M33) in testing distance indicators. The SMC appear to be so tidally disrupted that the line-of-sight differences in distance moduli across the system appears to be as large as 0.5 mag peak-to-peak.

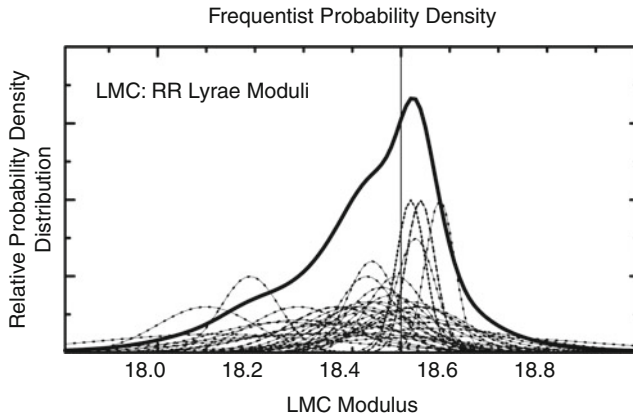
6 RR Lyrae Stars

It is probable that every type of variable star has been tested for its suitability as a distance indicator, if for no other reason than its period (if it has a stable period) or its characteristic timescale might be used as a distance-independent means of predicting the star's intrinsic luminosity. RR Lyrae stars are no exception to this rule, but they also have the added advantage that

many of them are known to be members of globular clusters. This latter attribute offers up the possibility that they can be independently calibrated in absolute terms, through main sequence fitting, for example. On the negative side, for most extragalactic applications, RR Lyrae variables are faint. They reside on the horizontal branch and have absolute magnitudes that are around $M_V = +0.5$ mag. An up-to-date and comprehensive review of the properties of RR Lyrae stars can be found in the monograph by Smith (1995), while a recent review of their status as distance indicators can be found in Bono (2003). An indication of the systematics encountered in applying RR Lyraes to the distance scale can be seen in [▶ Fig. 9-2](#), which compares 38 independent RR Lyrae distance determinations to the LMC.

Heroic ground-based efforts to detect RR Lyrae stars beyond the Magellanic Cloud were surpassed only in precision and sample size by HST. However, no effort by any telescope on the ground or in space has been made to detect RR Lyraes beyond the Local Group; they are simply too faint. Nevertheless 23 Local Group galaxies have been successfully surveyed for RR Lyrae stars; a representative sampling of these is given in [▶ Table 9-1](#).

If RR Lyraes are to be continued to be observed in Local Group galaxies and used to test for consistency in overlapping distance indicators, then there are some newly revealed advantages in moving the calibration to the near infrared. As modeled by Catelan et al. (2004) and earlier observed by Longmore et al. (1986), the period-luminosity relation for RR Lyrae stars becomes significantly better defined in the near infrared, having a steeper slope and much decreased intrinsic scatter, as compared to the optical where the V-band magnitude is almost degenerate with period. This behavior for variable stars in general is discussed in Madore and Freedman (2012).



■ Fig. 9-2

Thirty-eight RR Lyrae star distance determinations to the LMC. The modal value is 18.52 mag. *Dashed lines* are unit-area Gaussians whose mean is at the published distance and whose sigma corresponds to the published statistical error. Determinations without a published uncertainty were all assigned an uncertainty of 0.10 mag for plotting purposes only. The *solid line* represents the frequentist sum of these Gaussians. The *thin solid vertical line* marks a fiducial distance modulus of 18.50 mag acting as a point of reference when comparing subsequent plots

■ Table 9-1
RR Lyrae distances

Galaxy	(m-M) ± err	NED reference code
M31	23.23 ± 0.15	1988ApJ...331..135P
	23.35 ± 0.15	1987ApJ...316..517P
	23.46 ± 0.11	2009AJ....138..184S
	23.48 ± 0.11	2004AJ....127.2738B
	23.49 ± 0.19	2010ApJ...708..817F
	23.50 ± 0.10	2004AJ....127.2738B
	23.51 ± 0.11	2004AJ....127.2738B
	23.52 ± 0.08	2009ApJ...704L.103C
	23.59 ± 0.19	2010ApJ...708..817F
	23.64 ± 0.19	1988ApJ...331..135P
M33	24.67 ± 0.08	2006AJ....132.1361S
	24.47 ± 0.12	1992MmSAI..63..331L
	24.84 ± 0.16	2000AJ....120.2437S
NGC 147	23.85 ± 0.22	1987AJ.....94.1556S
	23.92 ± 0.25	1990AJ....100..108S
	24.16 ± 0.16	2010ApJ...708..293Y
NGC 205	24.65 ± 0.25	1992AJ....103..84S
NGC 6822	23.36 ± 0.17	2003ApJ...588L..85C
IC 10	24.56 ± 0.08	2008ApJ...688L..69S
IC 1613	24.10 ± 0.27	1992AJ....104.1072S
	24.30 ± 0.05	2003AJ....125.1261D
	24.32 ± 0.16	2001ApJ...550..554D
	24.44 ± 0.10	2010ApJ...712.1259B
	24.47 ± 0.12	2010ApJ...712.1259B
LMC	18.19 ± 0.06	1990AJ....100.1532W
	18.52 ± 0.02	2000AAp...363L...1K
	18.48 ± 0.08	2004AAp...423...97B
	18.61 ± 0.28	1999AAp...348L..33G
SMC	18.86 ± 0.07	1988AJ.....96..872W
	18.78 ± 0.15	1986MNRAS.221..887R
	18.86 ± 0.07	2003AJ....125.1261D
	18.93 ± 0.24	2004AJ....128..736W
And I	24.49 ± 0.06	2005AJ....129.2232P
And II	24.11 ± 0.02	2004AJ....127..318P
And III	24.38 ± 0.06	2005AJ....129.2232P
And VI	24.56 ± 0.06	2002AJ....124.1464P
Draco	19.40 ± 0.02	2004AJ....127..861B
Fornax	20.53 ± 0.09	2007ApJ...670..332G
	20.66 ± 0.03	2003MNRAS.345..747M
Leo A	24.52 ± 0.09	2003AJ....125.1261D
Sextans	24.52 ± 0.09	2003AJ....125.1261D
Sculptor	19.67 ± 0.02	2008AJ....135.1993P

■ Table 9-2

Galactic Cepheids with geometric parallaxes

Cepheid	P(days)	logP	μ (mag)	σ (%)	Distance (pc)
RT Aur	3.728	0.572	8.15	7.9	427
T Vul	4.435	0.647	8.73	12.1	557
FF Aql	4.471	0.650	7.79	6.4	361
δ Cep	5.366	0.730	7.19	4.0	274
Y Sgr	5.773	0.761	8.51	13.6	504
X Sgr	7.013	0.846	7.64	6.0	337
W Sgr	7.595	0.881	8.31	8.8	459
β Dor	9.842	0.993	7.50	5.1	316
ζ Gem	10.151	1.007	7.81	6.5	365
l Car	35.551	1.551	8.56	9.9	515

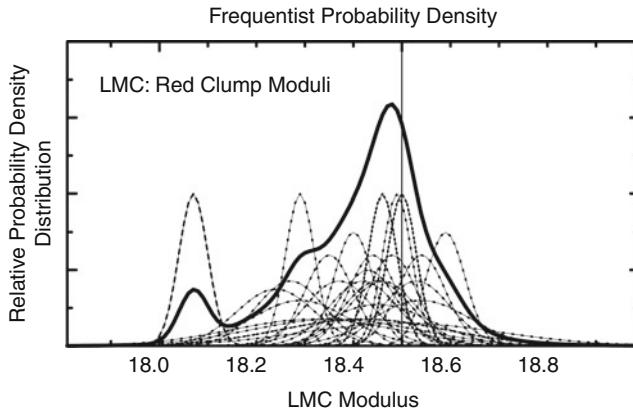
7 Red Clump Stars

After leaving the hydrogen-burning main sequence, stars can enter a second fairly long-lived phase of central nuclear energy generation, this time powered by core helium burning. The helium-burning main sequence of low-mass stars is seen as the horizontal branch typical of many Population II systems. The helium-burning main sequence of intermediate-age (higher-mass) clump stars can be seen in the color–magnitude diagram as an enhancement in the luminosity function near to the giant branch and at an absolute magnitude level slightly brighter than the older, traditional horizontal branch.

Use of the red giant clump as a distance indicator has had a checkered history. This is primarily due to the difficulty of establishing the age and metallicity of the underlying stellar populations, but it is also affected by the changing wavelength domain that has been used to calibrate it. The evolving nature of our understanding of this feature is best illustrated by its application to determining a distance to the LMC.

As with many distance indicators, age and metallicity effects are often in play at the same time, but the luminosity measured at different wavelengths may be responding, to varying degrees, to each of these effects. The question ultimately boils down to this: Is the luminosity of any given feature in the color–magnitude diagram a strong function of age and/or metallicity? Often a second parameter is usually sought to “calibrate out” the sensitivity of the luminosity to nuisance parameters such as metallicity and age (see, e.g., Alves and Sarajedini 1999; Girardi and Salaris 2001). However, it is also true that the degree to which any one of these parameters affects the luminosity can itself be a function of wavelength. Atmospheric line transitions that are often sensitive to and diagnostic of metallicity are heavily concentrated in the shorter-wavelength blue and optical portions of the spectrum; therefore by moving to the red or near infrared, one should become naturally less sensitive to metallicity and thus a better distance indicator. The other immediate benefit of moving as far to the infrared as possible is the monotonically decreasing effect of interstellar reddening.

Udalski et al. (1998) and later Udalski (2000) used I-band data for the red clump stars in the LMC to argue for a very small distance modulus to the LMC of 18.24 mag, or nearly 0.25 mag short of the generally accepted distance modulus of 18.50 mag. The debate rapidly gathered momentum and diverged on several fronts. Stanek et al. (1998) compared I-band



■ Fig. 9-3

Thirty-two Red Clump distance determinations to the LMC. The modal value is 18.52 mag (See RR Lyrae caption ● Fig. 9-2) for plotting details)

data of red clump stars from the Hipparcos catalog with their counterparts in two fields in the LMC and found an even shorter distance to the LMC corresponding to a true modulus of only $18.07 \text{ mag} \pm 0.03$ (random) ± 0.09 (systematic).

Alves (2000) then moved the debate to the near infrared by providing a K-band calibration based again on galactic stars with direct individual parallaxes from Hipparcos combined with I-band photometry. Koerwer (2009) subsequently applied a mid-IR calibration of the red clump to the LMC and found 18.54 ± 0.06 mag. Alves et al. (2002) and also Pietrzynski et al. (2003) each determined a distance modulus for the LMC that yielded a value of 18.50 ± 0.03 mag. The Alves calibration was claimed to be independent of metallicity over the range $-0.5 < [\text{Fe}/\text{H}] < 0.00$ dex. However, Girardi and Salaris (2001) have modeled corrections for population effects, involving age and metallicity, (see also Sarajedini 1999 and Pietrzynski et al. 2010 for complementary empirical approaches) and find corrections in the I band of 0.2 mag. For completeness, see also Seidel et al. (1987), Paczynski and Stanek (1998), Grocholski and Sarajedini (2002) and Sarajedini et al. (2002).

Sixteen distance determinations to the LMC using the red clump method have been published; their values range from 18.03 to 18.59 mag; their distribution is shown in ● Fig. 9-3. Eleven other galaxies, all in the Local Group, have also had their distances estimated by the red clump method.

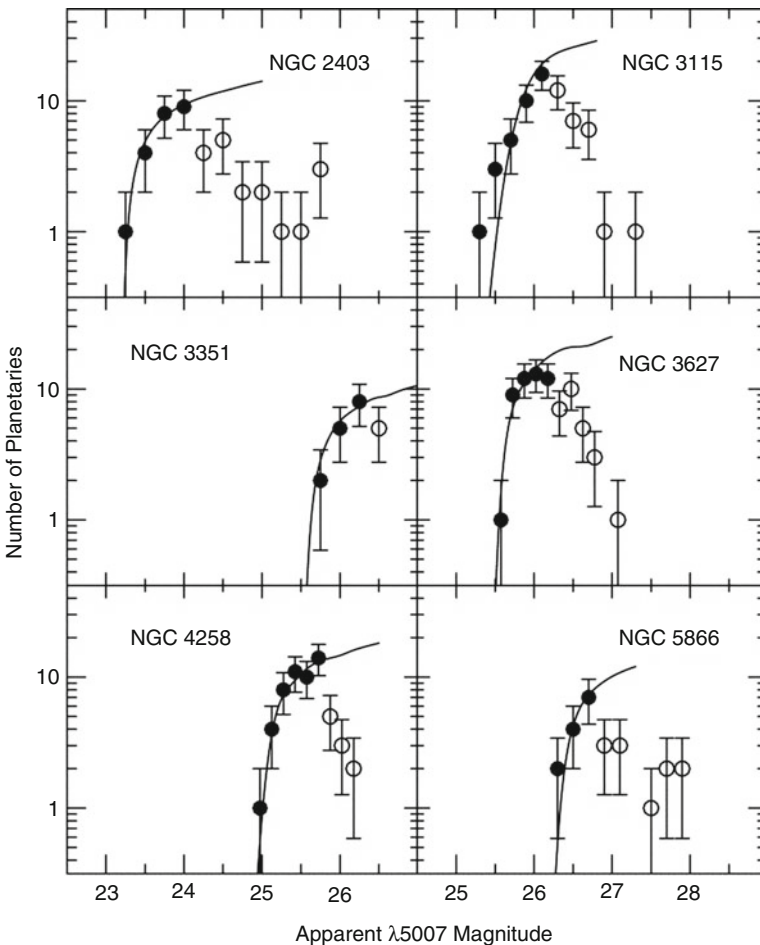
7.1 The CMD Method, the Horizontal Branch, and Mira Variables

Given full color-magnitude diagrams (CMD) for the resolved populations of nearby galaxies not only can individual stars (e.g., Cepheids, RR Lyraes, Miras, etc.) and featured groups of stars (such as the TRGB and the horizontal branch) be used to gauge distances, but the entire CMD itself can be deconstructed, with distances and stellar populations being self-consistently solved for. The concept finds its origins with Tolstoy and Saha (1996) and has been more fully developed by Dolphin (2002) and applied most recently by de Jong et al. (2008). Only eight

Local Group galaxies (And I, II, and III, Sculptor, CVn II, LGS 3, Ursa Minor, and Fornax) are close enough to use the horizontal branch method to determine distances. And four galaxies (LMC, M33, NGC 5128, and the Phoenix Dwarf) have been monitored sufficiently that they have had distance estimates derived from long-period Mira variables.

8 Planetary Nebula Luminosity Function (PNLF)

The distinctive and rapid cutoff observed at the bright end of the [OIII] λ 5007 emission-line luminosity function for planetary nebulae provides a distance determination method (e.g., Ciardullo et al. 1989). Examples of some luminosity functions obtained at the current distance limits of this method's application and the adopted fits are given in [Fig. 9-4](#). Extensively



■ Fig. 9-4

Examples of distance determination fits to planetary nebula luminosity functions (From Ciardullo et al. 2002)

referenced reviews of the technique can be found in Jacoby et al. (1992), Jacoby and Ciardullo (1993), and more recently Ciardullo (2003).

One important advantage of the PLNF method is that it can be applied to both elliptical galaxies and Population II rich spiral galaxies, thereby providing an important point of direct comparison of distance determination methods that are otherwise heavily restricted to only one or the other populations, such as the SBF method for elliptical galaxies and the Cepheid PL relation for spirals. An excellent reviews of PLNF distances are given in Ciardullo et al. (2002) and Ciardullo (2005).

There are some subtleties that need to be paid attention to in using the PLNF method for deriving distances. These include culling out interlopers, especially at the bright end of the luminosity function where the measurement of the edge is intrinsically sensitive to small-number statistics. Known contaminants include HII regions, supernova remnants, background high-redshift, emission-line galaxies, and rare but super-luminous planetary nebulae. Accounting for the possible effects of interstellar extinction is a concern not easily dealt with (Ciardullo et al. 2002).

To date, 57 galaxies have had their PNLF measured and used to estimate their distances; the most distant application being made to objects in the Virgo and Fornax clusters. Pressing the technique to large distances requires not only larger aperture telescopes but also custom-built (or tuneable) narrowband (30-Å) filters targeting specific redshift intervals appropriate to individual galaxies.

8.1 Globular Cluster Luminosity Functions (GCLF)

At one time, it was suggested that the brightest globular cluster in any given system might be used as a distance indicator (Sandage 1968). This proved not to be the case as later studies found that there was no bright cutoff in the globular cluster luminosity function (GCLF) and that the brightest globular clusters simply scaled with the size of the total population. Later the magnitude of the peak of the luminosity function, which is relatively bright ($M_V \sim -7.5$ mag), was explored as a distance indicator (Hanes 1979). Recent reviews and discussions of the GCLF method can be found in Tamman and Sandage (1999), Ferrarese et al. (2000), and Richler (2003). Further complications include the realization that cluster destruction rates will be different in disk galaxies compared to elliptical galaxies and will be a function of an individual cluster's physical structure, such as compactness. Gnedin and Ostriker (1998) calculate that 50–90% of a globular cluster population will be destroyed, by dynamical friction, tidal shocks, or simple core collapse and disintegration, in a Hubble time. Furthermore, the discovery of color bimodality in the integrated color–magnitude distributions of globular clusters in a number of nearby galaxies (see Forbes et al. 1997) means that there will be age or metallicity-induced differences in the mean magnitude of the luminosity function itself, thereby complicating its calibration and compromising its application as a distance indicator (see Richler 2003 for an in-depth discussion). To date, over 142 galaxies have their distances estimated by the GCLF method.

8.2 Novae

Novae are cataclysmic variables (thought to result from thermonuclear runaway on a mass-accreting white dwarf in a close binary system) whose absolute visual magnitudes cover

a wide range but can reach up to $M_V = -10$ mag. This alone makes them of interest as potential distance indicators. Zwicky (1936) was the first to note that the peak brightness of a nova correlates with its rate of decline; that is, intrinsically faint novae fade more slowly than their brighter counterparts. As most recently emphasized by Ferrarese et al. (2003), a calibration of the maximum magnitude versus rate of decline (MMRD) relation (actually called the “life-luminosity” relation by Zwicky) has proven to be “remarkably illusive,” primarily due to a lack of data. Other than M31, where the heroic surveys by Arp (1956) early on, and then again later by Capaccioli et al. (1989) produced many novae, the LMC (with only a handful of well-studied novae, Capaccioli et al. 1990) is the only other galaxy that has a viable sample of published light curves with which to attempt a calibration (e.g., Della and Livio 1995 for a recent example).

Novae cannot be predicted, but once found, they fade rapidly and are not easily followed up at other wavelengths or at higher signal-to-noise. Moreover, the interpretation of single-band discoveries is subject to being systematically compromised by unknown amounts of individual lines-of-sight extinction. A 24-orbit HST campaign to discover and follow novae in the Virgo-cluster galaxy, Messier 49 = NGC 4472 (Ferrarese et al. 2003), resulted in only five “fairly complete” light curves. However, the sobering conclusion of that study was that there are substantial differences in the shape of the MMRD in M31, the Milky Way, and M49. A more optimistic assessment of novae as extragalactic distance indicators can be found in Gilmozzi and Della Valle (2003) but see also Della and Livio (1995). Only three galaxies (LMC, M31, and M100 = NGC 4321) have had their distances estimated using novae.

8.3 Type II Supernovae: EPM and SEAM

Two methods are used to determine distances in the universe based on type II SN: the expanding photosphere method (EPM, Kirschner and Kwan 1974; Eastman and Kirshner 1989) and the spectral-fitting expanding atmosphere method (SEAM, Baron et al. 1995, 2004). The EPM is based on the Baade–Wesselink method (Baade 1926) and is particularly effective when the metallic line-blanketing effects in the optical are small (early phases). EPM uses a black-body approximation to the spectral energy distribution, adjust by a variety of correction factors (Eastman et al. 1996). SEAM uses synthetic spectra and fits the observed energy distributions directly. For a discussion of the relative merits of the two techniques, the reader is referred to the recent paper on the SN II distance scale (Dessart and Hiller 2005). Over 30 galaxies have had their distances determined using type II supernovae.

8.4 Cepheid Distance Scale

Since the discovery of the Leavitt Law (Leavitt 1908; Leavitt and Pickering 1912) and its use by Hubble to measure the distances to the Local Group galaxies, Cepheid variables have remained a widely applicable and powerful method for measuring distances to nearby galaxies. Cepheids’ periods of pulsation range from 2 to over 100 days, and their intrinsic brightnesses range from $-2 < M_V < -6$ mag. Detailed reviews of the Cepheid distance scale and its calibration can be found in Madore and Freedman (1991), Sandage and Tammann (2006), Fouque et al. (2007), and Barnes (2009). A recent, more lengthy discussion is contained in Freedman and Madore (2010), while a review of the early history of the subject is given in Fernie (1969).

There are many steps that must be taken in applying Cepheids to the extragalactic distance scale. Overcoming crowding and confusion is the key to the successful discovery, measurement, and use of Cepheids in galaxies beyond the Local Group. From the ground, atmospheric turbulence degrades the image resolution, decreasing the contrast of point sources against the background. As higher precision data have been accumulated for Cepheids in greater numbers and in different physical environments, it has become possible to search for and investigate a variety of lower level, but increasingly important, systematics affecting the Leavitt Law.

The physical basis for the Leavitt Law is well understood. Cepheid pulsation occurs because of the changing atmospheric opacity with temperature in the doubly ionized helium zone. This zone acts like a heat engine and valve mechanism. During the portion of the cycle when the ionization layer is opaque to radiation that layer traps energy resulting in an increase in its internal pressure. This added pressure acts to elevate the layers of gas above it, resulting in the observed radial expansion. As the star expands, it does work against gravity and the gas cools. As it does so, its temperature falls back to a point where the doubly ionized helium layer recombines and becomes transparent again, thereby allowing more radiation to pass. Without that added source of heating, the local pressure drops, the expansion stops, the star recollapses, and the cycle repeats. The alternate trapping and releasing of energy in the helium ionization layer ultimately gives rise to the periodic change in radius, temperature, and luminosity seen at the surface. Not all stars are unstable to this mechanism. The cool (red) edge of the Cepheid instability strip is thought to be controlled by the onset of convection, which then prevents the helium ionization zone from driving the pulsation. For hotter temperatures, the helium ionization zone is located too far out in the atmosphere for significant pulsations to occur. Further details can be found in the classic stellar pulsation textbook by Cox (1980), and Freedman and Madore (2010).

Cepheids have been intensively modeled numerically, with increasingly sophisticated hydrodynamical codes (for a recent review, see Buchler 2009). While continuing progress is being made, the challenges remain formidable in following a dynamical atmosphere and in modeling convection with a time-dependent mixing length approximation. In general, observational and theoretical period–luminosity–color relations are in reasonable agreement (e.g., Caputo 2008). However, subtle effects (e.g., that of metallicity on the luminosities and colors of Cepheids) remain difficult to predict from first principles.

8.4.1 Galactic Cepheids with Trigonometric Parallaxes

An accurate trigonometric parallax calibration for galactic cepheids has been long sought but very difficult to achieve in practice. All known classical (galactic) Cepheids are more than 250 pc away; therefore for direct distance estimates good to 10%, parallax accuracies of ± 0.2 milliarcsec are required, necessitating space observations. The HIPPARCOS satellite reported parallaxes for 200 of the nearest Cepheids, but (with the exception of Polaris) even the best of these had very low signal-to-noise ratio (Feast and Catchpole 1997).

Benedict et al. (2007) used the Fine Guidance Sensors (FGS) on HST to provide the first high-precision, geometric parallaxes to ten nearby galactic Cepheids having periods ranging from 4 to 36 days. *Spitzer* mid-infrared data for the HST parallax calibration sample, as well as Cepheids in the LMC, have now been obtained (Monson et al. 2012; Scowcroft et al. 2012; Freedman et al. 2012). The advantages of the mid-infrared are many, including the small dispersion in the mid-infrared Leavitt relations, as well as the insensitivity to reddening and metallicity.

9 The Distance to the Large Magellanic Cloud Based on Cepheids

Several thousand Cepheids have been identified and cataloged in the LMC (Leavitt 1908; Alcock et al. 2000; Soszynski et al. 2008), all at essentially the same distance. Both historically and today, the slope of the Leavitt Law is both statistically and systematically better determined in the LMC than it is for Cepheids in our own galaxy. This is especially true for the long-period end of the calibration where the extragalactic samples are much larger than the small sample of nearby Cepheids in the Milky Way. The main drawback to using the LMC as the fundamental calibrator of the Leavitt Law is the fact that the LMC Cepheids are of lower metallicity than many of the more distant spiral galaxies useful for measuring the Hubble constant. This systematic is largely eliminated by adopting the higher-metallicity galactic calibration or calibration based on the distance to the maser spiral galaxy, NGC 4258.

In [Fig. 9-5](#), we show the Leavitt Law at $3.6\ \mu\text{m}$ for 82 Cepheids in the LMC (with $6 < P < 60$ days) as given by Scowcroft et al. (2012). The dispersion in the $3.6\text{-}\mu\text{m}$ relation amounts to only $\pm 0.106\ \text{mag}$ (or an uncertainty of $\pm 5\%$ in distance for a single Cepheid). For comparison, we also show the V-band data from Madore and Freedman (1991) for LMC Cepheids. The dispersion in this case is more than a factor of 2 greater, amounting to $\pm 0.252\ \text{mag}$. One hundred previously published distance moduli to the LMC, based solely on Cepheids, are shown in [Fig. 9-6](#).

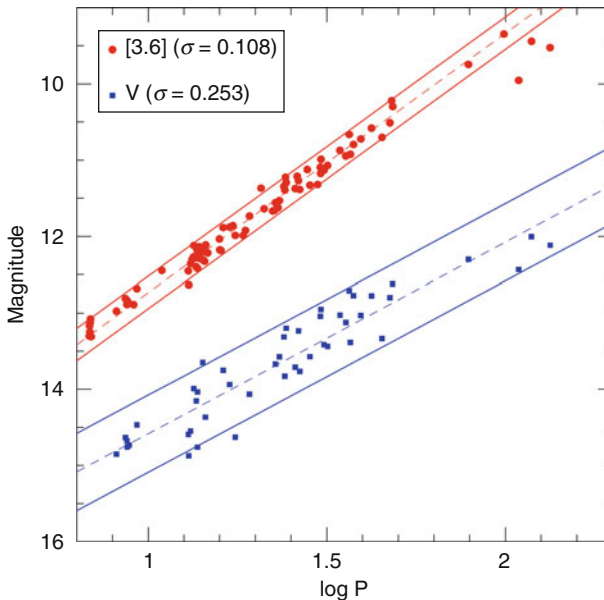
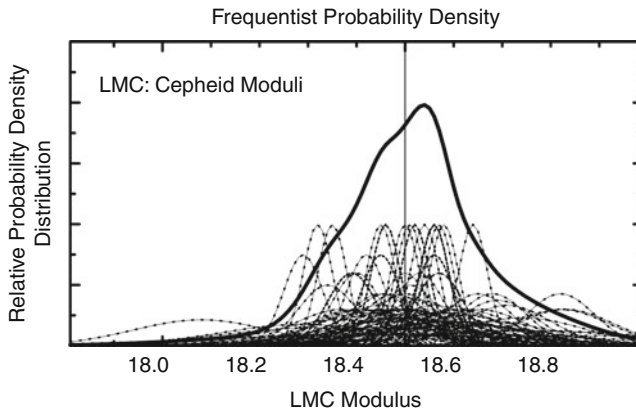


Fig. 9-5

Phase-averaged $3.6\text{-}\mu\text{m}$ (red circles) and V-band (blue squares) Leavitt Law relations for the LMC. The $3.6\text{-}\mu\text{m}$ data are from Scowcroft et al. (2012), the V-band from Madore and Freedman (1991). Note the small dispersion of $\pm 0.11\ \text{mag}$ at $3.6\ \mu\text{m}$, which is more than a factor of 2 less than for the V-band. The dashed lines represent weighted least square fits to the PL relations for Cepheids in the period range 6–60 days. The solid lines denote $2\text{-}\sigma$ ridge lines



■ Fig. 9-6

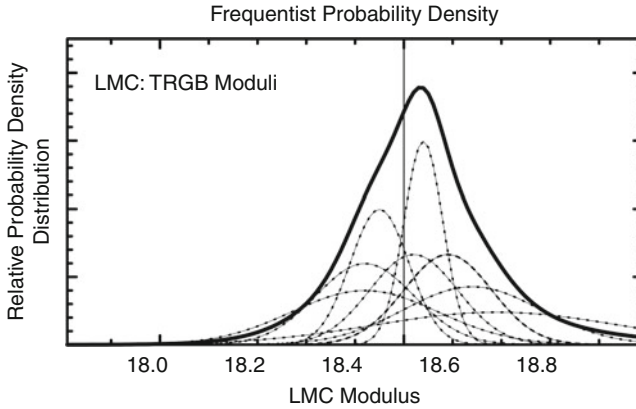
One hundred Cepheid distance moduli to the LMC. The modal value of the Cepheid distribution function falls at about 18.55 mag

9.1 Tip of the Red Giant Branch (TRGB) Method

The tip of the red giant branch (TRGB) method uses the theoretically well-understood and observationally well-defined discontinuity in the luminosity function of stars evolving up the red giant branch in old, metal-poor stellar populations. This feature has been calibrated using galactic globular clusters, and because of its simplicity and straightforward application, it has been widely used to determine distances to nearby galaxies. The method was developed quantitatively in two papers: one by DaCosta and Armandroff (1990) for galactic globular clusters and the other by Lee et al. (1993), where the use of a quantitative digital filter to measure the tip location was first introduced in an extragalactic context. The method has a precision comparable to Cepheids. Recent and excellent reviews of the topic have been published by Rizzi et al. (2007) and Bellazzini (2008).

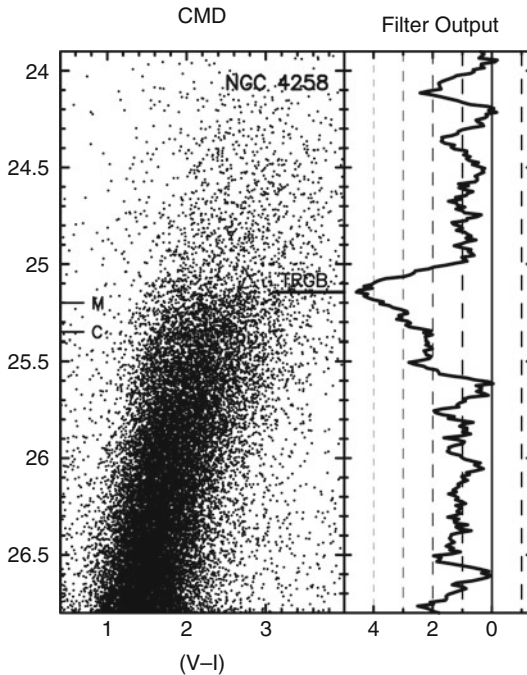
Approximately 250 galaxies have had their distances measured by the TRGB method. This is to be compared to a total of 57 galaxies with Cepheid distances. (A comprehensive compilation of direct distance determinations is available at the following website: <http://nedwww.ipac.caltech.edu/level5/NED1D/ned1d.html>). A comparison of nine applications of the TRGB method to the LMC is given in ▶ Fig. 9-7. In practice, the TRGB method is observationally a much more efficient technique since, unlike for Cepheid variables, there is no need to follow them through a variable light cycle; a single-epoch observation, made at two wavelengths (to provide color information), is sufficient. A recent example of applying the TRGB technique to the maser galaxy, NGC 4258, is shown in ▶ Figs. 9-7 and ▶ 9-8.

The TRGB is also well-understood theoretically (e.g., Iben and Renzini 1983; Freedman and Madore 2010). In brief, the helium core at the center of a red giant is supported by electron degeneracy pressure. A hydrogen-burning shell surrounds the core and provides the luminosity of the star. Fall-out, in the form of “helium ash” from the shell, increases the mass of the core over time. As the core mass increases, the radius shrinks, the temperature of the shell, and consequently the luminosity generated in the shell, increases; the star rises along the giant branch



■ Fig. 9-7

Nine tip of the red giant branch (TRGB) distance determinations to the LMC. The modal value is 18.53 mag. See RR Lyrae caption (● Fig. 9-2) for plotting details



■ Fig. 9-8

An example of the detection and measurement of the discontinuity in the observed luminosity function for red giant branch stars in the halo of the maser galaxy NGC 4258 (Mager et al. 2008). The color-magnitude diagram on the left has been adjusted for metallicity such that the TRGB is found at the same apparent magnitude independent of color/metallicity of the stars at the tip. The *right panel* shows the output of an edge-detection (modified Sobel) filter whose peak response indicates the TRGB magnitude and whose width is used as a measure of the random error on the detection

with increasing luminosity and higher core temperatures. When the (isothermal) core temperature reaches a physically well-defined temperature, helium ignites throughout the core. This helium core ignition lifts the electron degeneracy within the core. This dramatic change in the equation of state is such that the core flash is internally quenched in a matter of seconds. The core is inflated and settles down to a lower-luminosity, helium core-burning main sequence. The transition from the red giant to the horizontal branch occurs rapidly (within a few million years) so that observationally the TRGB can be treated as a physical discontinuity. Nuclear physics fundamentally controls the stellar luminosity at which the RGB is truncated, essentially independent of the chemical composition and/or residual mass of the envelope sitting above the core.

The radiation from stars at the TRGB is redistributed with wavelength as a function of the metallicity and mass of the envelope. Empirically it is found that the bolometric corrections are smallest in the *I*-band, and most recent measurements have been made at this wavelength. The small residual metallicity effect on the TRGB luminosity is well documented and can be empirically calibrated out (see Madore et al. 2009).

9.2 Maser Galaxies

H₂O (water) megamasers have been shown to provide an independent and potentially powerful means of accurately measuring extragalactic distances geometrically. Lo (2005) has reviewed both the physical nature of megamasers and their application to the extragalactic distance scale. The technique utilizes the mapping of 22.2 GHz water maser sources orbiting in the accretion disks of black holes in spiral galaxies with active galactic nuclei, where modeling of those disks assumes simple Keplerian motion. A rotation curve is derived for the major axis of the disk; proper motions are measured on the near side of the disk on the minor axis. Scaling the angular velocities across the line of sight to the absolute (radial) velocities along the line of sight yields the distance.

The method requires a sample of accretion disks that are relatively edge on (so that a rotation curve can be obtained from radial-velocity measurements) and a heating source such as x-rays or shocks to produce maser emission. The basic assumption is that the maser emission arises from trace amounts of water vapor ($<10^{-5}$ in number density) in very small density enhancements in the accretion disk and that they act as perfect dynamical test particles. The maser sources appear as discrete peaks in the spectrum or as unresolved spots in the images constructed from Very Long Baseline Interferometry (VLBI). Measurements of the acceleration ($a = V^2/r$) are obtained directly by monitoring the change of maser radial velocities over time from single-dish observations. Proper motions are obtained from observed changes in angular position in interferometer images. The approximately Keplerian rotation curve for the disk can then be modeled, allowing for warps and radial structures. The best studied galaxy, NGC 4258, at a distance of about 7 Mpc is still too close to provide a secure measurement of the Hubble constant on its own (i.e., free from local velocity-field perturbations), but it can serve as an invaluable independent check of the Cepheid zero-point calibration.

9.2.1 A Maser Distance to NGC 4258

VLBI observations of H₂O maser sources surrounding the active galactic nucleus of NGC 4258 reveal them to be in a very thin, differentially rotating, slightly warped disk. The Keplerian

velocity curve has deviations of less than 1%. The disk has a rotational velocity in excess of 1,000 km/s at distances on the order of 0.1 pc from the inferred super-massive ($10^7 M_{\odot}$) nuclear black hole. Detailed analyses of the structure of the accretion disk as traced by the masers have been published (e.g., Herrnstein et al. 1999; Humphreys et al. 2008, and references therein). Over time, it has been possible to measure both proper motions and accelerations of these sources and thereby allow for the derivation of two independent distance estimates to this galaxy. The excellent agreement of these two estimates supports the a priori adoption of the Keplerian disk model and gives distances of 7.2 ± 0.2 and 7.1 ± 0.2 Mpc, respectively.

Because of the simplicity of the structure of the maser system in NGC 4258 and its relative strength, NGC 4258 will remain a primary test bed for studying systematic effects that may influence distance estimates. Several problems may limit the ultimate accuracy of this technique, however. For example, because the masers are only distributed over a small angular part of the accretion disk, it is difficult to assess the importance of noncircular orbits. Of possible concern, eccentric disks of stars have been observed in a number galactic nuclei where the potential is dominated by the black hole, as is the case for NGC 4258. In addition, even if the disk is circular, it is not a given that the masers along the minor axis are at the same radii as the masers along the major axis. The self gravity of the disk also may need to be investigated and modeled since the maser distribution suggests the existence of spiral arms (Humphreys et al. 2008). Finally, radiative transfer effects may cause nonphysical motions in the maser images. Although the current agreement of distances using several techniques is comforting, having only one sole calibrating galaxy for this technique remains a concern, and further galaxies will be required to ascertain the limiting uncertainty in this method.

9.2.2 Other Distance Determinations to NGC 4258

The first Cepheid distance to NGC 4258 was published by Maoz et al. (1999) who found a distance of 8.1 ± 0.4 Mpc, scaled to an LMC-calibrated distance modulus of 18.50 mag. Newman et al. (2001) found a distance modulus of 29.47 ± 0.09 (random) ± 0.15 (systematic), giving a distance of $7.83 \pm 0.3 \pm 0.5$ Mpc. Macri et al. (2006) reobserved NGC 4258 discovering 281 Cepheids at BV and I wavelengths in two radially (and chemically) distinct fields. Their analysis gives a distance modulus of $29.38 \pm 0.04 \pm 0.05$ mag (7.52 ± 0.16 Mpc), if one adopts $\mu(LMC) = 18.50$ mag. Several more recent determinations of resolved-star (Cepheid and TRGB) distance moduli to NGC 4258 are in remarkably good agreement with the maser distance modulus. For instance, diBenedetto (2008) measures a Cepheid distance modulus of $29.28 \pm 0.03 \pm 0.03$ for NGC 4258 (corresponding to a distance of 7.18 Mpc); Benedict et al. (2007) find a distance modulus of 29.28 ± 0.08 mag; and Mager et al. (2008) also find a value of $29.28 \pm 0.04 \pm 0.12$ mag both from Cepheids and from the TRGB method. These latter studies are in exact agreement with the current maser distance. Higher accuracy has come from larger samples with higher signal-to-noise data and improved treatment of metallicity.

An alternative approach to utilizing the maser galaxy in the distance scale is to adopt the geometric distance to NGC 4258 as foundational, use it to calibrate the Leavitt Law, and from there, determine the distance to the LMC. Macri et al. (2006) adopted this approach and concluded that the true distance modulus to the LMC is 18.41 ± 0.10 mag.

9.2.3 NGC 4258, UGC 3789, and Their Calibration of H_0

The distance to NGC 4258 has been used to bypass the LMC in calibrating the Cepheid PL relation and then secondary methods. For example, Macri et al. (2006) and Riess et al. (2009a, b) have adopted the distance to NGC 4258 to calibrate the supernova distance scale, as discussed further in [Sect. 10](#).

Attempts to measure distances to additional megamaser host galaxies have been challenging. About 2000 galaxies have been surveyed in search of nuclear disk masers, with about 100 masers being culled from this sample. The rather low detection rate of 5% is likely due to detection sensitivity, combined with the geometric constraint that the maser disk be viewed nearly edge on, because the maser emission is expected to be highly beamed in the plane of the disk. About 30 of these masers have spectral profiles indicative of emission from thin disks: that is, masers at the galactic systemic velocity and groups of masers symmetrically spaced in velocity. In the end, about a dozen maser galaxies are sufficiently strong that they are candidates for being imaged with phase-referenced VLBI techniques. However, only about five have been found to have sufficiently simple structures that they can be fit to dynamical models and thereby have their distances determined. The most promising example is UGC 03789 at a recessional velocity of 3,325 km/s. A first-epoch determination of a geometric distance to this galaxy has been published by Braatz et al. (2010) as part of the *Megamaser Cosmology Project* (Reid et al. 2009). For its geometric/maser distance of 49.9 ± 7.0 Mpc, this galaxy alone gives $H_0 = 69 \pm 11$ km/s/Mpc. Correcting the observed velocity for large-scale flow perturbations due to Virgo, the Great Attractor and the Shapley Concentration give $V = 3,530 \pm 26$ km/s and $H_0 = 71$ km/s/Mpc.

If a significant number of maser galaxies can be found and precisely observed even further into the Hubble flow, this method can, in principle, compete with methods such as SNe Ia for directly measuring distances at cosmologically significant scales.

9.3 Surface Brightness Fluctuation (SBF) Method

For distances to elliptical galaxies and early-type spirals with large bulge populations, the surface brightness fluctuation (SBF) method, first introduced by Tonry and Schneider (1988), overlaps with and substantially exceeds the current reach of the TRGB method (Tonry et al. 2001). Both methods use properties of the red giant branch luminosity function to estimate distances. The SBF method quantifies the effect of distance on an overall measure of resolution of the Population II red giant stars, naturally weighted both by their intrinsic luminosities and relative numbers. What is measured is the pixel-to-pixel variance in the photon statistics (scaled by the surface brightness) as derived from an image of a pure population of red giant branch stars. For fixed surface brightness, the variance in a pixel (of fixed angular size) is a function of distance simply because the total number of discrete sources contributing to any given pixel increases with the square of the distance. While the TRGB method relies entirely on the very brightest red giant stars, the SBF method uses a luminosity-weighted integral over the entire RGB population in order to define a typical “fluctuation star” whose mean magnitude, \overline{M}_I , is assumed to be universal and can therefore be used to derive distances. For recent discussions of the SBF method, the reader is referred to Biscardi et al. (2008), Blakeslee et al. (2009), and an update by Blakeslee et al. (2010).

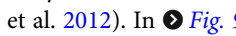
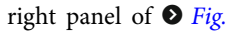
Aside from the removal of obvious sources of contamination such as foreground stars, dust patches, and globular clusters, the SBF method does require some additional corrections.

It is well known that the slope of the red giant branch in the color–magnitude diagram is a function of metallicity, and so the magnitude of the fluctuation star is both expected and empirically found to be a function metallicity. A (fairly steep) correction for metallicity has been derived and can be applied using the mean color of the underlying stellar population $\overline{M}_I = -1.74 + 4.5(V - I)_o - 1.15$ (Tonry et al. 2002).

9.4 Tully–Fisher Relation

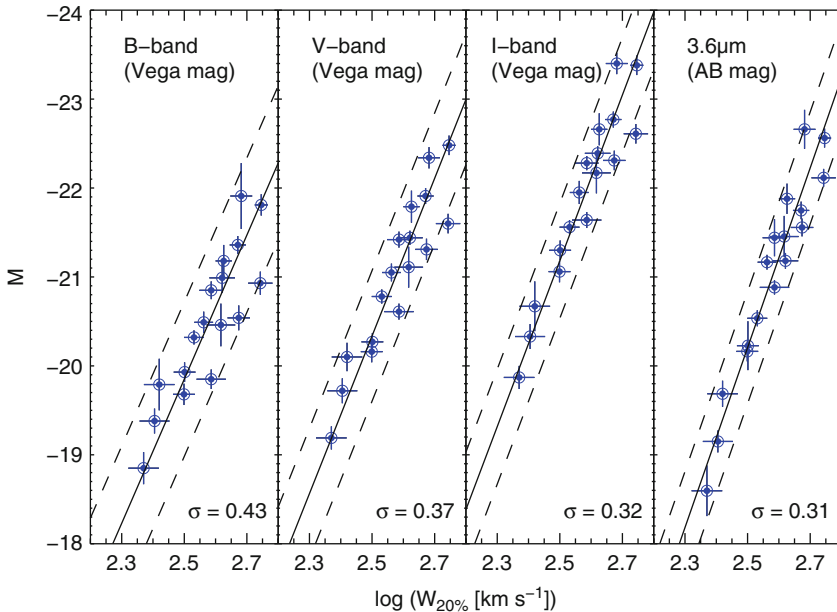
The total luminosity of a spiral galaxy (corrected to face-on inclination to account for extinction) is strongly correlated with the galaxy’s maximum (corrected to edge-on inclination) rotation velocity. This relation, calibrated via the Leavitt Law or TRGB, becomes a powerful means of determining extragalactic distances (Tully and Fisher 1977; Aaronson et al. 1986; Pierce and Tully 1988; Giovanelli et al. 1997). The Tully–Fisher relation at present is one of the most widely applied methods for distance measurements, providing distances to thousands of galaxies both in the general field and in groups and clusters. The scatter in this relation is wavelength-dependent and approximately ± 0.3 – 0.4 mag or 15–20% in distance (Giovanelli et al. 1997; Sakai et al. 2000; Tully and Pierce 2000).

In a general sense, the Tully–Fisher relation can be understood in terms of the virial relation applied to rotationally supported disk galaxies, under the assumption of a constant mass-to-light ratio (Aaronson et al. 1979). However, a detailed self-consistent physical picture that reproduces the Tully–Fisher relation (e.g., Steinmetz and Navarro 1999) and the role of dark matter in producing almost universal spiral galaxy rotation curves (McGaugh et al. 2000) still remain a challenge.

Spitzer archival data have recently yielded an unexpected and exciting discovery. Of the 23 nearby galaxies with HST Cepheid distances that can be used to independently calibrate the Tully–Fisher relation, there are 17 that currently also have 3.6- μm total magnitudes (Seibert et al. 2012). In  [Fig. 9-9](#) (left three panels), we show the B-, V-, and I-band TF relations for the entire sample of currently available calibrating galaxies from Sakai et al. (2000). Their magnitudes have been corrected for inclination-induced extinction effects, and their line widths have been corrected to edge-on. The scatter is ± 0.43 , 0.36, and 0.36 mag for the B-, V-, and I-band relations, respectively; the outer lines follow the mean regression at ± 2 sigma. In the right panel of  [Fig. 9-7](#), we show the mid-IR TF relation for the same 17 galaxies with Cepheid distances and IRAC observations, measured here at 3.6 μm . The scatter at 3.66 μm is ± 0.31 mag. This calibration will be applied to *Spitzer* 3.6- μm data for several hundred galaxies (Seibert et al. 2012).

9.5 Type Ia Supernovae

One of the most accurate means of measuring cosmological distances out into the Hubble flow utilizes the peak brightness of type Ia supernovae (SNe Ia). The potential of supernovae for measuring distances was clear to early researchers (e.g., Baade, Minkowski, Zwicky), but it was the Hubble diagram of Kowal (1968) that set the modern course for this field, followed by decades of work by Sandage, Tammann, and collaborators (e.g., Sandage and Tammann 1982; Sandage and Tammann 1990); see also the review by Branch (1998). Analysis by Pskovskii (1984), followed by Phillips (1993), established a correlation between the magnitude of an SN Ia

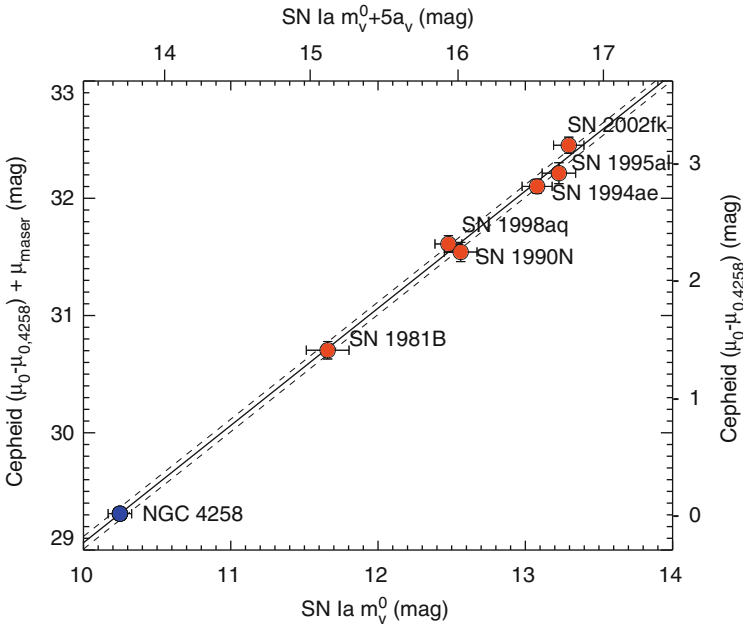


■ Fig. 9-9

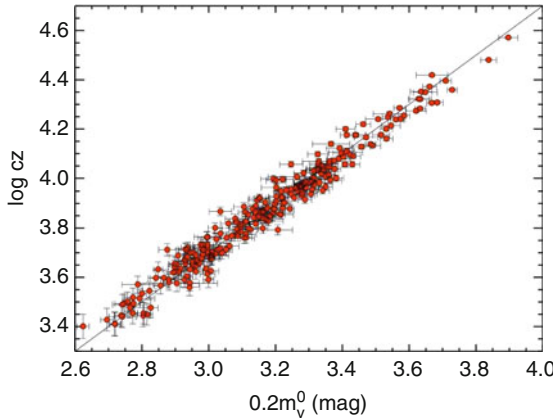
Multiwavelength Tully–Fisher relations. The three *left panels* show the B-, V-, and I-band TF relations for galaxies calibrated with independently measured Cepheid moduli at the end of the HST Key Project. W is the inclination-corrected line width (from Sakai et al. 2000) measured at the 20% power point. The *right-hand panel* shows the TF relation for the subset of galaxies drawn from the Key Project calibrators with measured 3.6- μm total AB magnitudes from Seibert et al. (2012). Data for 17 galaxies are available at all four wavelengths. The dispersions in these relations are shown in the *lower right*

at peak brightness and the rate at which it declines, thus allowing supernova luminosities to be “standardized.” This method currently probes farthest into the unperturbed Hubble flow, and it possesses very low intrinsic scatter; in recent studies, the decline-rate corrected SN Ia Hubble diagram is found to have a dispersion of $\pm 7\text{--}10\%$ in distance (e.g., Folatelli et al. 2010; Hicken et al. 2009). A simple lack of Cepheid calibrators prevented the accurate calibration of type Ia supernovae for determination of H_0 prior to HST. Substantial improvements to the supernova distance scale have resulted from recent dedicated, ground-based supernova search and follow-up programs yielding CCD light curves for nearby supernovae (e.g., Hamuy et al. 1996; Jha et al. 2006; Contreras et al. 2010). Sandage and collaborators undertook a major program with HST to find Cepheids in nearby galaxies that have been host to Type Ia supernovae (Sandage et al. 1996; Saha et al. 1999), and thereby provided the first Cepheid zero-point calibration, which has recently been followed up by Macri et al. (2006) and Riess et al. (2009a, b) ● Figs. 9-10 and ● 9-11.

SNe Ia result from the thermonuclear runaway explosions of stars. From observations alone, the presence of SNe Ia in elliptical galaxies suggests that they do not come from massive stars. Many details of the explosion are not yet well understood, but the generally accepted view is that of a carbon–oxygen, electron-degenerate, nearly Chandrasekhar mass white dwarf orbiting in



■ Fig. 9-10
 A comparison of Cepheid and SNe Ia distances (*red points*), as described in Riess et al. (2009b). The calibrating galaxy, NGC 4258, is added in *blue*



■ Fig. 9-11
 Supernova Hubble diagram based on 240 supernovae with $z < 0.1$. The sample is from Hicken et al. (2009) and has been used by Riess et al. (2009b) for their determination of H_0

a binary system with a close companion (Whelan and Iben 1973). As material from the Roche lobe of the companion is deposited onto the white dwarf, the pressure and temperature of the core of the white dwarf increase until explosive burning of carbon and oxygen is triggered. An alternative model is that of a “double degenerate” system (merger with another white dwarf).

Although on observational grounds, there appear to be too few white dwarf pairs, this issue has not been conclusively resolved. A review of the physical nature of SNe Ia can be found in Hillebrandt and Niemeyer (2000).

A defining characteristic of observed SNe Ia is the lack of hydrogen and helium in their spectra. It is presumed that the orbiting companion is transferring hydrogen- and helium-rich material onto the white dwarf; however, despite extensive searches, this hydrogen or helium has never been detected, and it remains a mystery as to how such mass transfer could take place with no visible signature. It is not yet established whether this is a problem of observational detection or whether these elements are lost from the system before the explosion occurs.

Various models for SN Ia explosions have been investigated. The most favored model is one in which a subsonic deflagration flame is ignited, which subsequently results in a supersonic detonation wave (a delayed detonation). The actual mechanism that triggers an SN Ia explosion is not well understood: successfully initiating a detonation in a CO white dwarf remains extremely challenging. In recent years, modeling in 3D has begun, given indications from spectropolarimetry that the explosions are not spherically symmetric. The radiative transport calculations for exploding white dwarf stars are complex. However, there is general consensus that the observed (exponential shape of the) light curves of SNe Ia are powered by the radioactive decay of ^{56}Co to ^{56}Fe . The range of observed supernova peak brightnesses appears to be due to a range in ^{56}Ni produced. However, the origin of the peak magnitude – decline rate – is still not well understood.

Despite the lack of a solid theoretical understanding of SNe Ia, empirically they remain one of the best-tested, lowest-dispersion, and highest-precision means of measuring relative distances out into the smooth Hubble flow.

10 The Extragalactic Distance Scale and the Hubble Constant

We now give a brief discussion of the application of the extragalactic distance scale to measurements of the Hubble constant and its uncertainties. A recent, detailed review of the Hubble constant can be found in Freedman and Madore (2010). We focus here on recent efforts, subsequent to that of the Hubble Space Telescope Key Project (Freedman et al. 2001).

A recent calibration of SNe Ia has come from Riess et al. (2009a, b, 2011) from a new calibration of six Cepheid distances to nearby well-observed supernovae using the Advanced Camera for Surveys (ACS) and the Near-Infrared Camera and Multi-Object Spectrometer (NICMOS) on HST. By extending to the near-infrared, these observations of the newly discovered Cepheids directly address the systematic effects of metallicity and reddening. Riess et al. determine a value of $H_0 = 74.2 \pm 3.6 \text{ km s}^{-1} \text{ Mpc}^{-1}$ combining the systematic and statistical errors. This value is in excellent agreement with that from the Key Project (Freedman et al. 2001), which is calibrated using the galactic Cepheid parallax sample. At the current time, there is not much need for larger, low-redshift samples since the dominant remaining uncertainties are systematic rather than statistical. Recent studies (e.g., Wood-Vasey et al. 2008; Folatelli et al. 2010) confirm that supernovae are better standard candles at near-infrared (JHK) wavelengths and minimize the uncertainties due to reddening.

Tammann et al. (2008) also undertook a recent recalibration of supernovae, as well as a comparison of the Cepheid, RR Lyrae, and TRGB distance scales. In contrast, they find a

value of $H_0 = 62.3 \pm 4.0 \text{ km s}^{-1} \text{ Mpc}^{-1}$, where the quoted (systematic) error includes their estimated uncertainties in both the Cepheid and TRGB calibration zero points. Their quoted error is dominated by the systematic uncertainties in the Cepheid zero point and the small number of supernova calibrators, both of which are estimated by them to be at the 3–4% level; however, the H_0 values differ by more than $2\text{-}\sigma$. A discussion of the reason for the differences in these analyses can be found in Riess et al. (2009a, b); these include the use of more heavily reddened galactic Cepheids, the use of less accurate photographic data, and a calibration involving multiple telescope/instruments for supernovae by Tammann, Sandage, and Reindl.

A recent and comprehensive review of the application of the SBF method to determining cosmic distances, and its comparison to the fundamental plane (FP) method is given in Blakeslee et al. (2002). This analysis leads to the a value of $H_0 = 72 \pm 4(\text{random}) \pm 11(\text{systematic}) \text{ km s}^{-1} \text{ Mpc}^{-1}$. Mould and Sakai (2008) have used the TRGB as an alternate calibration to the Cepheid distance scale for the determination of H_0 . They use 14 galaxies for which TRGB distances can be measured to calibrate the Tully–Fisher relation, and determine a value of $H_0 = 73 \pm 5$ (statistical only) $\text{ km s}^{-1} \text{ Mpc}^{-1}$, a value about 10% higher than found earlier by Sakai et al. (2000) based on a Cepheid calibration of 23 spiral galaxies with Tully–Fisher measurements. In subsequent papers, they calibrate the SBF method (Mould and Sakai 2009a) and the FP for early-type galaxies and the luminosity scale of type Ia supernovae (Mould and Sakai 2009b). They conclude that the TRGB and Cepheid distance scales are all consistent using SBF, FP, SNe Ia, and the TF relation.

As part of a new Carnegie Hubble Project (CHP), new mid-infrared observations of Cepheids have been obtained at $3.6\text{ }\mu\text{m}$ using the *Spitzer Space Telescope* (Freedman et al. 2012). A mid-IR zero point of the Leavitt Law is obtained using time-averaged $3.6\text{-}\mu\text{m}$ data for the five longest-period, high-metallicity (Milky Way) Cepheids having trigonometric parallaxes (Monson et al. 2012). The slope is measured from new time-averaged, mid-IR data for 82 Large Magellanic Cloud Cepheids falling in the period range $0.8 < \log(P) < 1.8$ (Scowcroft et al. 2011). These data yield a value of $H_0 = 74.3 \pm 1.5$ (statistical) ± 2.1 (systematic) km/s/Mpc (Freedman et al. 2012). This *Spitzer* calibration decreases the systematic uncertainty in H_0 over that obtained by the Hubble Space Telescope Key Project by a factor of 3.

Mid-infrared observations retire many of the systematic uncertainties in the Cepheid distance scale, which dominate at optical wavelengths. Specifically, the mid-IR reduces, by a factor of at least 20, the sensitivity of the Cepheid distance scale to reddening corrections and assumptions about the universality of the reddening law. The new *Spitzer* calibration eliminates instrumental zero-point uncertainties for the Cepheids, as it is based solely on observations taken using a single, stable detector/telescope combination (the *Spitzer* IRAC camera). This calibration is also less sensitive to metallicity effects since it is centered on a high-metallicity (galactic) zero point. Moreover, the $3.6\text{-}\mu\text{m}$ band is demonstrably less sensitive to the atmospheric metallicity effects seen at shorter wavelengths. The current systematic uncertainty on the Hubble constant is now dominated by the small number of galactic calibrators having independent, trigonometric distances. This systematic error will be significantly reduced with the inclusion of addition Cepheid parallaxes expected to be forthcoming from the Global Astrometric Interferometer for Astrophysics (GAIA) mission. In principle, a value of H_0 having a well-tested and robust systematic error budget of only 2% is within reach over the next decade.

Acknowledgments

Many dedicated individuals have contributed to the progress in accurately calibrating the extragalactic distance scale; it has been a community effort spanning the better part of a century. The authors made extensive use of the *NASA/IPAC Extragalactic Database* (NED) in preparing this chapter.

References

- Aaronson, M., Huchra, J. P., & Mould, J. R. 1979, *ApJ*, 229, 1
- Aaronson, M., Bothun, G., Mould, J., Huchra, J., Schommer, R. A., & Cornell, M. E. 1986, *ApJ*, 302, 536
- Albrecht, A., Bernstein, G., Cahn, R., Freedman, W. L., Hewitt, J., et al. 2006, *astro-ph/0609591*
- Alcock, C., Allsman, R. A., Alves, D. R., Axelrod, T. S., et al. 2000, *AJ*, 119, 2194
- Alloin, D., & Gieren, W. 2003, in *Stellar Candles for the Extragalactic Distance Scale*, Lecture Notes in Physics, ed. D. Alloin, & W. Gieren (Heidelberg: Springer), 635, 1
- Alves, R. D. 2000, *ApJ*, 539, 732
- Alves, R. D. 2004, *New AR*, 48, 659
- Alves, R. D., & Sarajedini, A. 1999, *ApJ*, 511, 225
- Alves, R. D., Rejkuba, M., Minniti, D., & Cook, K. H. 2002, *ApJL*, 573, 51
- Arp, H. C. 1956, *AJ*, 61, 15
- Baade, W. 1926, *AN*, 228, 359
- Barnes, T. G. 2009, in *Stellar Pulsation: Challenges for Theory and Observation*, AIP Conference Proceedings, Vol. 1170, ed. J. A. Guzik, & P. A. Bradley (Melville: American Institute of Physics), 3
- Baron, E., Hauschildt, P. H., Branch, D., et al. 1995, *ApJ*, 441, 170
- Baron, E., Nugent, P. E., Branch, D., & Hauschildt, P. H. 2004, *ApJ*, 616, L91
- Bellazzini, M. 2008, *Mem. Soc. Astron. Ital.* 79, 440
- Benedict, G. F., McArthur, B. E., Feast, M. W., Barnes, T. G., Harrison, T. E., et al. 2007, *ApJ*, 79, 453
- Biscardi, I., Raimondo, G., Cantiello, M., & Brocato, E. 2008, *ApJ*, 678, 168
- Blakeslee, J. P., Lucey, J. R., Tonry, J. L., Hudson, M. J., Narayanan, V. K., & Barris, B. J. 2002, *MNRAS*, 330, 443
- Blakeslee, J. P., Jordan, A., Mei, S., Cote, P., Ferrarese, L., et al. 2009, *ApJ*, 694, 556
- Blakeslee, J. P., Cantiello, M., Mei, S., Cote, P., DeGraaff, R. B., Ferrarese, L., et al. 2010, *ApJ*, 724, 657
- Bono, G. 2003, in *Stellar Candles for the Extragalactic Distance Scale*, Lecture Notes in Physics, Vol. 635, ed. D. Alloin, & W. Gieren (Heidelberg: Springer), 85
- Braatz, J. A., Reid, M. J., Humphreys, E. M., Henkel, C., Condon, J. J., & Lo, K. Y. 2010, *ApJ*, 718, 657
- Branch, D. 1998, *ARAA*, 36, 17
- Brunthaler, A., Reid, M. J., Falcke, H., Greenhill, M. J., & Henkel, C. 2005, *Science*, 307, 1440
- Buchler, J. R. 2009, in *Stellar Pulsation, Challenges for Theory and Observation*, ed. J. Guzik, & P. Bradley. AIP Conference Proceedings, Vol. 1170, 51. *astro-ph/0907.1766*
- Capaccioli, M., della Valle, M., Rossino, L., & D'Onofrio, M. 1989, *AJ*, 97, 1622
- Capaccioli, M., della Valle, M., D'Onofrio, M., & Rosino, L. 1990, *ApJ*, 360, 63
- Caputo, F. 2008, *Mem. Soc. Astron. Ital.* 79, 453
- Catelan, M., Pritzl, B. J., & Smith, H. A. 2004, *ApJS*, 154, 633
- Ciardullo, R. 2003, in *Stellar Candles for the Extragalactic Distance Scale*, Lecture Notes in Physics, Vol. 635, ed. D. Alloin, & W. Gieren (Heidelberg: Springer), 243
- Ciardullo, R. 2005, in *Planetary Nebulae as Astronomical Tools*, AIP Conference Proceedings, Vol. 804, ed. R. Szczerba, G. Stasinska, & S. K. Gorny (Melville: American Institute of Physics), 277
- Ciardullo, R., Jacoby, G. H., Ford, H. C., & Neill, J. D. 1989, *ApJ*, 339, 53
- Ciardullo, R., Feldmeier, J. J., Jacoby, G. H., Kuzio de Naray, R., Laychak, M. B., et al. 2002, *ApJ*, 577, 31
- Contreras, C., Hamuy, M., Phillips, M. M., Folatelli, G., Suntzeff, N. B., et al. 2010, *AJ*, 139, 519
- Cox, J. P. 1980, *Theory of Stellar Pulsation* Princeton: Princeton University Press
- Da Costa, G. S., & Armandroff, T. E. 1990, *AJ*, 100, 162
- Darling, J. 2011, *ApJL*, 732, 2
- de Grijs, R. 2011, *An Introduction to Distance Measurement in Astronomy* (Chichester: Wiley)

- de Jong, J. T. A., Rix, H., Martin, N. F., Zucker, D. B., Dolphin, A. E., Bell, E. F., Belokurov, V., & Evans, N. W. 2008, *AJ*, 135, 1361
- Della Valle, M., & Livio, M. 1995, *ApJ*, 452, 704
- Dessart, L., & Hillier, D. J. 2005, *A&A*, 439, 671
- di Benedetto, G. P. 2008, *MNRAS*, 390, 1762
- Dolphin, A. E. 2002, *MNRAS*, 332, 91
- Eastman, R. G., & Kirshner, R. P. 1989, *ApJ*, 347, 771
- Eastman, R. G., Schmidt, B. P., & Kirshner, R. 1996, *ApJ*, 466, 911
- Feast, M. W., & Catchpole, R. M. 1997, *MNRAS*, 286, L1
- Fernie, J. D. 1969, *PASP*, 81, 707
- Ferrarese, L., et al. 2000, *ApJ*, 529, 745
- Ferrarese, L., Cote, P., & Jordan, A. 2003, *ApJ*, 612, 1261
- Folatelli, G., Phillips, M. M., Burns, C. R., Contreras, C., Hamuy, M., et al. 2010, *AJ*, 139, 120
- Forbes, D. A., Brodie, J. P., & Grillmair, C. J. 1997, *AJ*, 113, 1652
- Fouque, P., Arriagada, P., Storm, J., Barnes, T. G., Nardetto, N., et al. 2007, *A&A*, 476, 73
- Freedman, W. L., & Madore, B. F. 2010, *ARAA*, 48, 673
- Freedman, W. L., Madore, B. F., Monson, A., Persson, S. E., Scowcroft, V., Seibert, M., & Rigby, J. 2012, *ApJ*, 758, 24
- Freedman, W. L., Madore, B. F., Gibson, B. K., Ferrarese, L., Kelson, D. D., et al. 2001, *ApJ*, 553, 47
- Freedman, W. L., Madore, B. F., Rigby, J., Persson, S. E., & Sturch, L. 2008, *ApJ*, 679, 71
- Gascoigne, S. C. B., & Shobbrook, R. R. 1978, *PASA*, 3, 285
- Gilmozzi, R., & Della Valle, M. 2003, in *Stellar Candles for the Extragalactic Distance Scale, Lecture Notes in Physics*, Vol. 635, ed. D. Alloin, & W. Gieren (Heidelberg: Springer), 229
- Giovanelli, R., Haynes, M. P., Herter, T., Vogt, N. P., da Costa, L. N., et al. 1997, *AJ*, 113, 53
- Girardi, L., & Salaris, M. 2001, *MNRAS*, 323, 109
- Gnedin, O. Y., & Ostriker, J. P. 1998, in *Galactic Halos*, ASP Conference Series, Vol. 136, ed. D. Zaritsky, 56
- Grocholski, A. J., & Sarajedini, A. 2002, *AJ*, 123, 1603
- Hamuy, M., Phillips, M. M., Suntzeff, N. B., Schommer, R. A., Maza, J., et al., 1996, *AJ*, 112, 2398
- Hanes, D. A. 1977, *MNRAS*, 180, 309
- Hanes, D. A. 1979, A new determination of the Hubble Constant, *MNRAS*, 188, 901
- Heck, A., & Caputo, F. 1999, *Post-Hipparcos Cosmic Candles*, A&SSL (Dordrecht: Kluwer)
- Henkel, C., Wouterloot, J. G. A., & Bally, J. 1986, *A&A*, 155, 193
- Herrnstein, J. R., Moran, J. M., Greenhill, L. J., Diamond, P. J., Inoue, M., et al. 1999, *Nature*, 400, 539
- Hicken, M., Wood-Vasey, W. M., Blondin, S., Challis, P., Jha, S., et al. 2009, *ApJ*, 700, 1097
- Hillebrandt, W., & Niemeyer, J. C. 2000, *ARAA*, 38, 191
- Hodge, P. 1982, *ARAA*, 19, 357
- Hubble, E. E. 1925, *ApJ*, 62, 409
- Hubble, E. P. 1926, *ApJ*, 63, 236
- Hubble, E. P. 1929, *ApJ*, 69, 103
- Huchra, J. P. 1992, *Science*, 256, 321
- Humphreys, E. M. L., Reid, M. J., Greenhill, L. J., Moran, J. M., & Argon, A. L. 2008, *ApJ*, 672, 800
- Iben, I., & Renzini, A. 1983, *ARAA*, 21, 271
- Jackson, N. 2007 *Living Rev. Relativ.* 10, 4
- Jacoby, G. H., Branch, D., Ciardullo, R., Davies, R. L., Harris, W. E., et al. 1992, *PASP*, 104, 599
- Jacoby, G. H., & Ciardullo, R. 1993, in *Planetary Nebulae, Proceedings IAU Symposium*, Vol. 155, ed. R. Weinberger, & A. Acker (Dordrecht/Boston: Kluwer), 503
- Jameson, R. F. 1986, *Vistas Astron.*, 29, 17
- Jha, S., Kirshner, R. P., Challis, P., Garnavich, P. M., Matheson, T., et al. 2006, *AJ*, 131, 527
- Jones, W. C., Ade, P. A. R., Bock, J. J., Bond, J. R., Borrill, L., et al. 2006, *ApJ*, 647, 823
- Kirshner, R. P., & Kwan, J. 1974, *ApJ*, 193, 27
- Koerwer, J. F. 2009, *AJ*, 138, 1
- Komatsu, E., Dunkley, J., Nolta, M. R., Bennett, C. L., Gold, B., et al. 2009, *ApJS*, 180, 330
- Kowal, C. T. 1968, *AJ*, 73, 1021
- Leavitt, H. S. 1908, *Ann. Harv. Coll. Obs.*, 60, 87
- Leavitt, H. S., & Pickering, E. C. 1912, *Harv. Coll. Obs. Circ.*, 173, 1
- Lee, M. G., Freedman, W. L., & Madore, B. F. 1993, *ApJ*, 417, 553
- Livio, M., Donahue, M., & Panagia, N. 1999, *The Extragalactic Distance Scale, STScI Symposium*, No. 10 (Cambridge: Cambridge University Press)
- Lo, K. Y. 2005, *ARAA*, 43, 625
- Loeb, A., Reid, M. J., & Falke, H. 2005, *ApJ*, 633, 894
- Longmore, A. J., Fernley, J. A., & Jameson, R. F. 1986, *MNRAS*, 220, 279
- Macri, L. M., Stanek, K. Z., Bersier, D., Greenhill, L. J., & Reid, M. J. 2006, *ApJ*, 652, 1133
- Madore, B. F., & Freedman, W. L. 1991, *PASP*, 103, 933
- Madore, B. F., & Freedman, W. L. 2012, *ApJ*, 744, 132
- Madore, B. F., Mager, V., & Freedman, W. F. 2009, *ApJ*, 690, 389
- Mager, V., Madore, B. F., & Freedman, W. F. 2008, *ApJ*, 689, 721
- Maiz, E., Newman, J. A., Ferrarese, L., Stetson, P. B., Zepf, S. E., et al. 1999, *Nature*, 401, 351

- McGaugh, S. S., Schombert, J. M., Bothun, G. D., & de Blok, W. J. G. 2000, *ApJL*, 533, L99
- Monson, A., Freedman, W. L., Madore, B. F., et al. 2012, *ApJ*
- Mould, J., & Sakai, S. 2008, *ApJL*, 686, L75
- Mould, J., & Sakai, S. 2009a, *ApJ*, 694, 1331
- Mould, J., & Sakai, S. 2009b, *ApJ*, 697, 996
- Mould, J. R., Huchra, J. P., Freedman, W. L., Kennicutt, R. C., Ferrarese, L., et al. 2000, *ApJ*, 529, 786
- Newman, J. A., Ferrarese, L., Stetson, P. B., Maoz, E., Zepf, S. E., et al. 2001, *ApJ*, 553, 562
- Nolta, M., Dunkley, J., Hill, R. S., Hinshaw, G., Komatsu, E., et al. 2009, *ApJS*, 180, 296
- Paczynski, B., & Stanek, K. Z. 1998, *ApJL*, 494, 219
- Perryman, M. A. C. 2009, *Astronomical Applications of Astrometry: Ten Years of Exploitation of the Hipparcos Satellite Data* (Cambridge: Cambridge University Press)
- Phillips, M. M. 1993, *ApJL*, 413, L105
- Pierce, M. J., & Tully, R. B. 1988, *ApJ*, 330, 579
- Pietrzynski, G., Gieren, W., & Udalski, A. 2003, *AJ*, 125, 2494
- Pietrzynski, G., Gorski, M., Gieren, W., Laney, D., Udalski, A., & Ciechanowski, A. 2010, *AJ*, 140, 1038
- Pskovskii, Y. P. 1984, *Sov. AJ*, 28, 658
- Readhead, A. C. S., Mason, B. S., Contaldi, C. R., Pearson, T. J., Bond, J. R., et al. 2004, *ApJ*, 609, 498
- Reichardt, C., Ade, P. A. R., Bock, J. J., Bond, J. R., Brevik, J. A., et al. 2009, *ApJ*, 694, 1200
- Reid, M. J., Braatz, J. A., Condon, J. J., Greenhill, L. J., Henkel, C., et al. 2009, *ApJ*, 695, 287
- Richler, T. 2003, in *Stellar Candles for the Extragalactic Distance Scale*, Lecture Notes in Physics, Vol. 635, ed. D. Alloin, & W. Gieren (Heidelberg: Springer), 281
- Riess, A. G., Macri, L., Casertano, S., Sosey, M., Lampeitl, H., et al. 2009a, *ApJ*, 699, 539
- Riess, A. G., Macri, L., Li, W., Lampeitl, H., Casertano, S., et al. 2009b, *ApJS*, 183, 109
- Riess, A. G., Macri, L., Casertano, S., Lampeitl, H., Ferguson, H. C., Filippenko, A. V., Jha, S. W., Li, W., & Chornock, R. 2011, *ApJ*, 730, 119
- Rizzi, L., Tully, R. B., Makarov, D., Makarova, L., Dolphin, A. E., et al. 2007, *ApJ*, 661, 81
- Rowan-Robinson, M. 1985, *The Cosmological Distance Ladder, Distance and Time in the Universe* (New York: W. H. Freeman)
- Saha, A., Sandage, A. R., Tammann, G. A., Labhardt, L., Macchetto, F. D., et al. 1999, *ApJ*, 522, 802
- Sakai, S., Mould, J. R., Hughes, S. M. G., Huchra, J. P., Macri, L. M., et al. 2000, *ApJ*, 529, 698
- Sandage, A. R. 1968, *ApJL*, 152, 149
- Sandage, A. R., Saha, A., Tammann, G. A., Labhardt, L., Panagia, N., & Macchetto, F. D. 1996, *ApJL*, 460, 15
- Sandage, A. R., & Tammann, G. A. 1982, *ApJ*, 265, 339
- Sandage, A. R., & Tammann, G. A. 1990, *ApJ*, 365, 1
- Sandage, A. R., & Tammann, G. A. 2006, *ARRA*, 44, 93
- Sarajedini, A., 1999, *AJ*, 118, 2321
- Sarajedini, A., Grocholski, A. J., Levine, J., & Lada, E. 2002, *AJ*, 124, 2625
- Scowcroft, V., Freedman, W. L., Madore, B. F., Monson, A. J., Persson, S. E., Seibert, M., Rigby, J. R., & Sturch, L. 2011, *ApJ*, 743, 76
- Scowcroft, V., Freedman, W. L., Madore, B. F., Monson, A., Persson, E., Seibert, M., Rigby, J., Stetson, P., & Sturch, L. 2012, *ApJ*, 747, 84
- Schaeffer, B. 2008, *AJ*, 135, 112
- Seibert, M., Freedman, W. L., Madore, B. F., Monson, A., Persson, E., Scowcroft, V. M., Rigby, J., Stetson, P., & Sturch, L. 2012, *ApJ*
- Seidel, E., Da Costa, G. S., & Demarque, P. 1987, *ApJ*, 313, 192
- Smith, R. 1982, *The Expanding Universe, Astronomy's Great Debate 1900–1931* (Cambridge: Cambridge University Press)
- Smith, H. A. 1995, *RR Lyrae Stars, Cambridge Astrophysics Series*, Vol. 27 (Cambridge/New York: Cambridge University Press)
- Soszynski, I., Poleski, R., Udalski, A., Szymanski, M. K., Kubiak, M., et al. 2008, *Acta. Astron.* 58, 163
- Stanek, K. Z., Zaritsky, D. & Harris, J. 1998, *ApJ*, 500, L141
- Steinmetz, M., & Navarro, J. 1999, *ApJ*, 513, 555
- Tammann, G. A., & Sandage, A. 1999, in *Harmonizing Cosmic Distance Scales in a Post-Hipparcos Era*, ASP Conference Series, Vol. 167, ed. D. Egret, & A. Heck (San Francisco: Astronomical Society of the Pacific), 204
- Tammann, G. A., Sandage, A. R., & Reindl, B. 2008, *A&AR*, 15, 289
- Tolstoy, E., & Saha, A. 1996, *ApJ*, 462, 672
- Tonry, J., & Schneider, D. P. 1988, *AJ*, 96, 807
- Tonry, T. J., Dressler, A., Blakeslee, J. P., Ajhar, E. A., Fletcher, A. B., Luppino, G. A., Metzger, M. R., & Moore, C. B. 2001, *ApJ*, 546, 681
- Tonry, T. J., Blakeslee, J. P., Ajhar, E. A., & Dressler, A. 2002, *ApJ*, 530, 625
- Tully, R. B., & Fisher, J. R. 1977, *A&A*, 54, 661
- Tully, R. B., & Pierce, M. J. 2000, *ApJ*, 553, 744
- Udalski, A., 2000, *Acta Astron.*, 50, 279
- Udalski, A., Szymanski, M., Kubiak, M., et al. 1998, *Acta Astron.*, 48, 147
- van den Bergh, S. 1992, *PASP*, 104, 861

- van den Bergh, S., & Pritchet, C. (eds.) 1988, *The Extragalactic Distance Scale*, ASP Conference Series, Vol. 4. (San Francisco: Astronomical Society of the Pacific)
- Webb, S. 1999, *Measuring the Universe* (Praxis: Springer)
- Weinberg, M. D., & Nikolaev, S. 2001, *ApJ*, 548, 712
- Whelan, J., & Iben, I. J. 1973, *ApJ*, 186, 100
- Wilcots, E. M., & Miller, B. W. 1998, *AJ*, 116, 2363
- Wood-Vasey, W. M., Friedman, A. S., Bloom, J. S., Hicken, M., Modjaz, M., et al. 2008, *ApJ*, 689, 377
- Zwicky, F. 1936, *PASP*, 48, 191